Journal of the European Ceramic Society 20 (2000) 159–168

Corrosion mechanisms of low porosity ZrO_2 based materials during near net shape steel casting

C.G. Aneziris*, E.M. Pfaff, H.R. Maier

Institute for Ceramic Components in Mechanical Engineering, RWTH Aachen, Nizzaallee 32, 52072 Aachen, Germany

Received 23 September 1998; received in revised form 9 April 1999; accepted 11 May 1999

Abstract

One of the most promising refractory materials for application in near net shape steel casting technologies is zirconia. The corrosion resistance of zirconia based materials in contact with steel and aggressive high casting speed powders has been investigated in a specially designed device simulating operating conditions; the corrosion mechanisms have been illustrated. © 2000 Elsevier Science Ltd. All rights reserved.

Zussamenfassung

Zirkondioxid weist sehr vorteilhafte Korrosionseigenschaften für Anwendungen in endabmessungsnahen Stahlstranggießtechnolo-gien auf. In einer speziell konstruierten Versuchsanordnung, wo die Betriebsbedingungen simuliert wurden, konnten die Korrosionsbeständigkeit von Zirkondioxidmaterialien in Kontakt mit Stahl und Hochgießgeschwindigkeitspulvern untersucht und die Korrosionsmechanismen erläutert werden. © 2000 Elsevier Science Ltd. All rights reserved.

Résumé

La zircone montre les meilleurs propriétés des materiaux réfractaires disponibles à l'usage de la technologie de la coulée continue d'acier à mesure exacte. Pour simuler des conditions de service un montage expérimental spécial a été construit. Avec celui-ci la résistance à la corrosion des materiaux composés de zircone a été examinée en contact avec l'acier et les poudres de coulée ultrarapides. Les mécanismes de la corrosion ont été expliqués. © 2000 Elsevier Science Ltd. All rights reserved.

Keywords: Steel castings; Corrosion; ZrO_2; Refractories

1. Introduction

As a new generation of continuous casting, near net shape steel processing, with its basic versions of thin slab casting and strip casting has been rapidly developed in the last decade; refractory materials have met the greatest challenge in order to attain the advanced metal quality as well as economical and ecological criteria.

In order for near net shape casting to reach the same degree of productivity as conventional continuous casting, it is necessary to use casting speeds ten times greater than in the conventional process.[1] Therefore a moving mould is generally employed in near net shape casting.[2] Ceramics have to meet technical requirements such as the sealing of molten steel in a moving mould exposed to aggressive high casting speed powders. High corrosion resistance combined with sufficient thermal shock resistance are required for reliable ceramic components such as submerged nozzles, slide gates and linings of refining vessels.[3, 4]

The most critical ceramic component in the tundish area reflects in the best way the difficulties that occur during the design of refractory materials for near net shape processing; this is the submerged nozzle.[5] The combination of ordinary carbon bonded Al_2O_3- or ZrO_2-nozzles that have been used in the past in conventional continuous casting plants no longer fulfil the demands for high corrosion resistance. More aggressive powders are being used and furthermore components with thin walls are needed, in order to give to the flowing metal the free space between the walls of the mould for quality reasons.[6]

The best available ceramic material for steel casting with regard to high corrosion and erosion resistant

* Corresponding author.

PII: S0955-2219(99)00149-1

performance is ZrO_2.[7] Zirconia porous refractories for applications in continuous casting are based on coarse and fine grained zirconia. A third group of materials which has not yet come into use in the steel industry, is dense zirconia. This last material as an engineering ceramic exhibits good mechanical properties and excellent corrosion resistance against steel/slag systems. The disadvantage of the dense structure is the high sensitivity to thermal shock. With special preheating arrangements and thin wall design however thermal shock attack can be controlled.[8,9]

Several papers[10–13] have described the corrosion mechanisms of carbon bonded Al_2O_3 materials during continuous steel casting, whereby three main attack locations appear: the ceramic/air/slag interface, the ceramic/steel/slag interface and the steel bath. A partial dissolution of the graphite in the slag resulting from the flow and pressure conditions (Marangoni-flow) occuring between the interfaces, has been proposed as the principle corrosion mechanism.[14]

For zirconia based materials, little attention has been given to the modern continuous casting technologies in terms of the corrosion attack of the highly aggressive casting powders.

It is well known that the tetragonal-monoclinic phase transformation and the associated volume change preclude the use of unstabilised zirconia in the bulk form.[15] In most refractory cases MgO partial stabilised zirconia is used.[16] According to the ZrO_2–MgO phase diagram there is a little or no solubility of MgO in monoclinic zirconia up to the tetragonal transformation temperature, where the solubility increases slowly up to 1%, Fig. 1. A cubic solid solution becomes stable above 1400°C with a eutectoid composition at 13% mol MgO.[17] A feature of technological importance is the cubic and tetragonal solid solution phase field.

In many cases of partially stabilised MgO–zirconia, the tetragonal phase can be recognised as spheroids or lenses of approximately 50–500 nm contained in big cubic grains or at their grain boundaries, where the tetragonal "lenses" are aligned at right angles.[18,19] During thermal, chemical, mechanical or particle size destabilisation, a martensitic phase transformation takes place (tetragonal to monoclinic).

At high temperatures stabilised zirconia can although amphoteric and comparatively stable to both acid and basic slags and glasses be destabilised on prolonged contact with either siliceous or alumino silicate compounds. The destabilisation of MgO partially stabilised zirconia is enhanced by the presence of SiO_2, TiO_2, Fe_2O_3 and Al_2O_3, whereby SiO_2 dominates by removing the MgO from the zirconia crystal and producing magnesium silicates at the grain boundaries.[20]

In a specially designed device[21,22] simulating the operating conditions of thin slab casting, several low porosity zirconia based materials have been examined in terms of their corrosion resistance; corrosion mechanisms have been proposed.

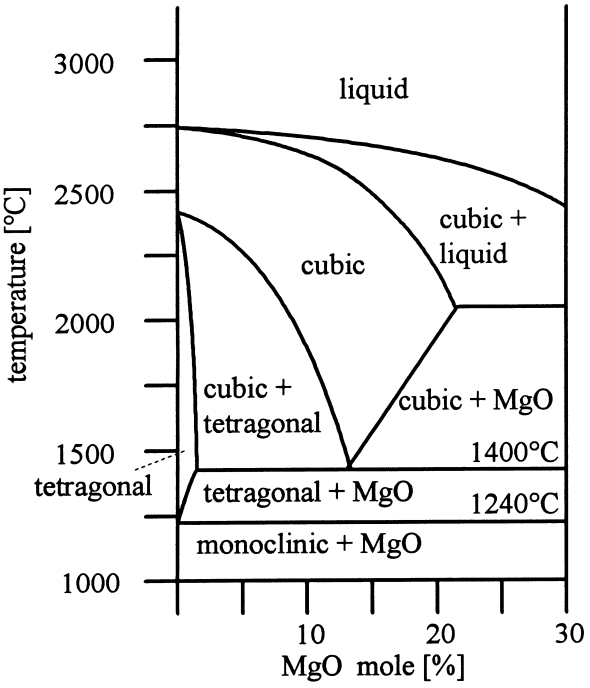

Fig. 1. The ZrO_2 rich section of the ZrO_2-MgO phase diagram.[17]

2. Experimental methods

MgO (3.5 wt%) partially stabilised zirconia (Unitec) with different grain size distributions varying between 0–12 μm for slip cast products and 10–2000 μm for isostatic pressed components has been used. Pilot submerged nozzles (thickness 4 to 15 mm, width 40 to 50 mm and length 250 mm) have been produced by slip casting and cold isostatic pressing. Especially the slip casting technique enables the manufacturing of thin wall components that are needed for near net shape casting technologies. Material A and B have been sintered at 1600°C for 2 h in air and material C has been fired at 900°C for 4 h in vacuum. In Table 1 the material properties are listed.

Fig. 2 shows the schematic of a corrosion testing device simulating the operating conditions of submerged nozzles including the oscillation of the mould and relative movement of the steel and the slag against the submerged nozzle. The rotation (60 rotations through 90°/min) and the oscillation (lift 10 mm, 60 oscillations/min) of the testing device have been tuned according to the conditions observed for conventional submerged materials during operation in steel plants. Specimens, 120×25–30×5–10 mm, have been cut out of the pilot submerged nozzles and have been placed in ceramic crucibles of MgO partially stabilised dense

Table 1
Material properties

	Material (wt%)	Processing route	Grain size d_{50} before firing (μm)	Open porosity (%)	Total porosity (%)	Material characterisation
A	100% MgO (3.5 wt%) Partial stab. ZrO_2	Slip casting	2–4	2	6	Sintered zirconia, dense, fine
B	100% MgO (3.5 wt%) Partial stab. ZrO_2	Slip casting	7–9	15	18	Sintered zirconia, porous, fine
C	80% MgO (3.5 wt%) Partial stab. ZrO_2, 20% C	Cold isostatic pressing	60	16	18	Carbon bonded zirconia, porous, coarse

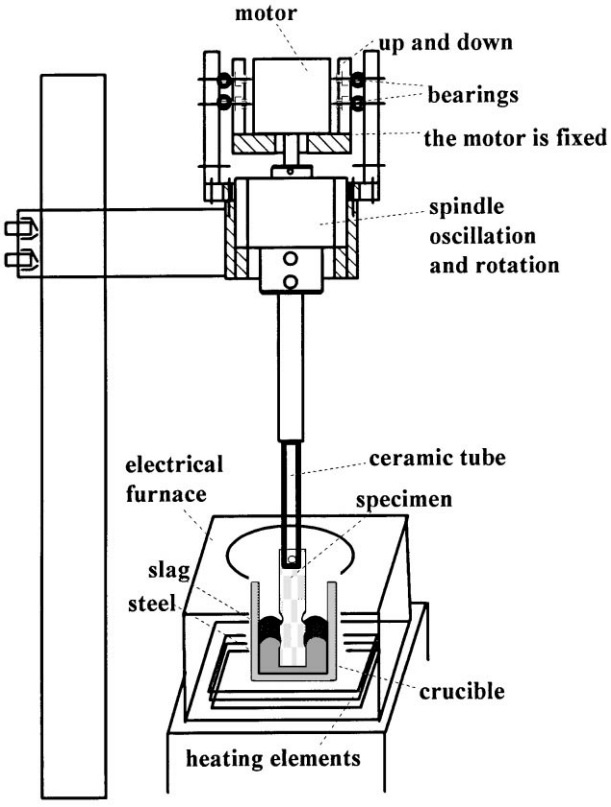

Fig. 2. Experimental testing arrangement for corrosion attack simulating the operating conditions of thin slab casting.

Table 2
Corrosion rates of zirconia based materials at the three main corrosive regions

Corrosion rate (mm/h)	Region I interface ceramic/steel/slag	Region II interface ceramic/air/slag	Region III steel bath
Material A, dense, fine	0.20	0.10	–
Material B, porous, fine	0.60	0.40	–
Material C, porous, coarse	3.00	0.30	–

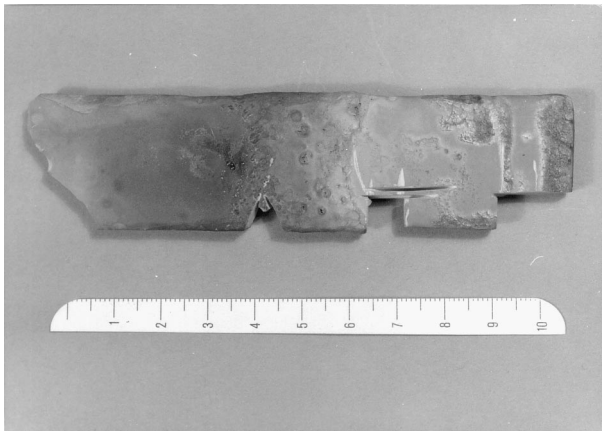

Fig. 3. Material A (dense zirconia) after corrosion test at 1550°C for 120 min, region I at positions 8.7–9.7, region II at positions 6.3–7.4 and region III at position 10.

zirconia filled with 600 g steel ST37 and 300 g high casting speed powder (30 wt% SiO_2, 30 wt% CaO, 10 wt% Al_2O_3, 5 wt% F^-, 6–8 wt% Na_2O-K_2O, 10–12 wt% C_{total}). In Table 2 the corrosion rates (measuring the difference of the widths before and after corrosion) of the tested materials after 120 min at 1550°C are listed.

The corrosion process was studied with the aid of optical as well as SEM techniques. Probes of the tested specimens of the three main attack regions have been cut out (see Fig. 3) and SEM micrographs of the broken and polished surfaces have been prepared. Because of the indication of diffusion of the slag elements in the inner area, EDX line scans have been carried out. Furthermore, the phase composition (monoclinic, tetragonal and cubic) of the different attacked regions versus the width has been measured by XRD[23,24] (Table 3, material A).

3. Experimental results and discussion

The corrosion attack of the three zirconia specimens is described by similar basic mechanisms.

In Fig. 4 a macroscopic picture of the corroded materials A and C is presented. The corrosion resistance of the dense material is remarkable at all three regions (ceramic/steel/slag interface-region I, ceramic/air/slag interface-region II and steel bath-region III) in comparison to the carbon bonded one (see also Table 2).

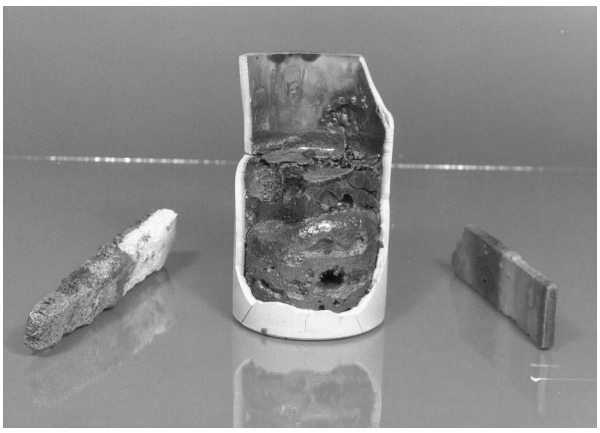

Fig. 4. Corrosion test at 1550°C for 120 min, left carbon bonded zirconia (mat. C), middle crucible with solidified slag and steel and right dense zirconia (mat. A).

In Fig. 5 the dense material is shown prior to the corrosion attack. Small pores of 2–3 μm are observed on the grain boundaries of 12–15 μm cubic zirconia grains, Fig. 6. Furthermore the tetragonal phase with size of 0.5–1 μm can be observed in the cubic grains. The cubic phase contains nanoporosity of approximately 50–100 nm.

In Fig. 7 a schematic diagram indicating the different regions of corrosive behaviour of material A is presented. In Fig. 8 a polished cross-section of the region ceramic/steel/slag can be seen. The corrosion attack at the outer surface runs straight, while some dendrite zirconia structures have remained partially dissolved in the slag. Observing normal to the polished inner surface (Fig. 9, approximately 200 μm in from the outer surface) the microstructure has been disaggregated, slag

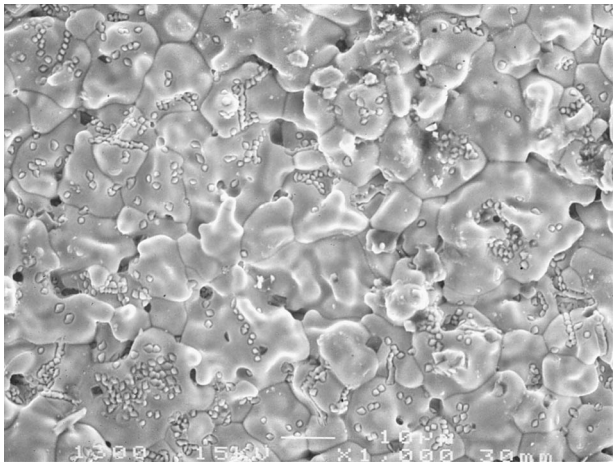

Fig. 5. Surface of dense zirconia (mat. A), SEM micrograph.

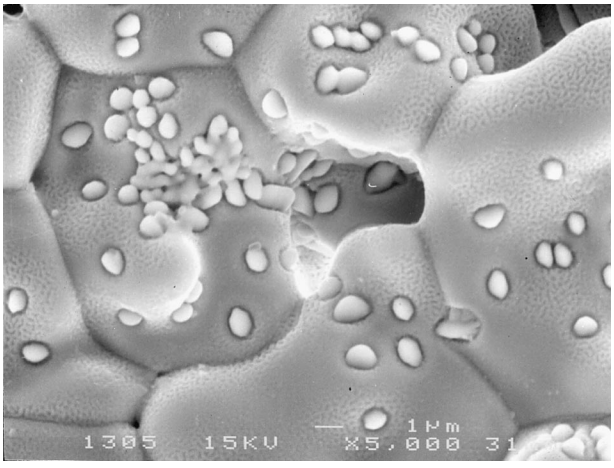

Fig. 6. Dense zirconia (mat. A) with tetragonal grains (0.5–1 μm) in the cubic grains (12–15 μm).

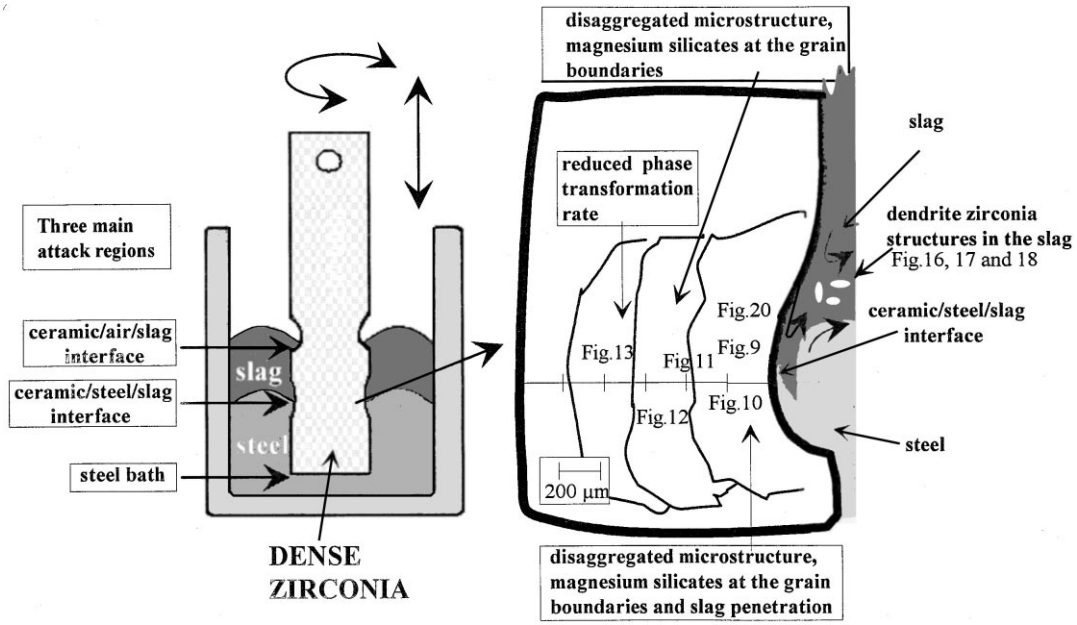

Fig. 7. Schematic diagram indicating the different regions of corrosive behaviour of material A.

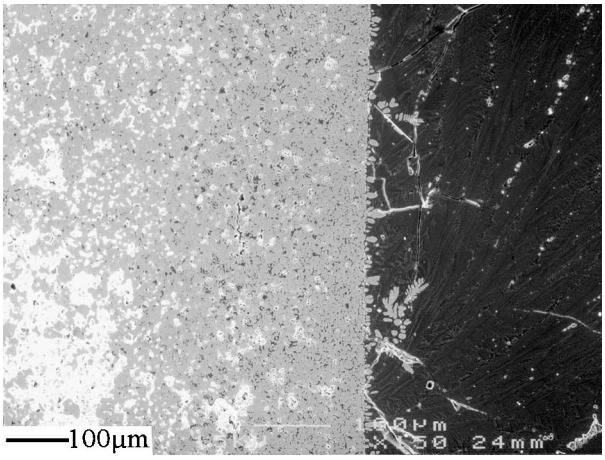

Fig. 8. Cross section of polished surface, dense zirconia (mat. A) after corrosion test at 1550°C for 120 min, region I.

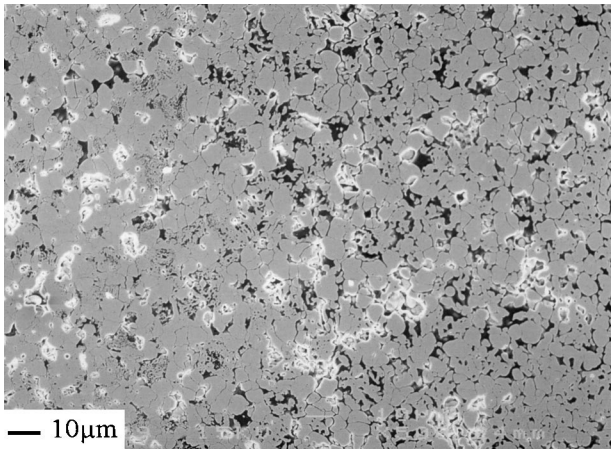

Fig. 9. Polished inner surface, 200 μm from the outer area, dense zirconia (mat. A) after corrosion test at 1550°C for 120 min, region I.

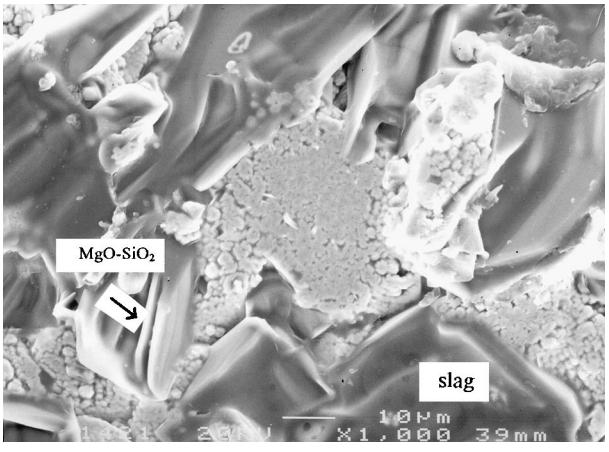

Fig. 10. Magnesium silicates and slag around monoclinic grains, 200 μm from the outer area, dense zirconia (mat. A) after corrosion test at 1550°C for 120 min, region I.

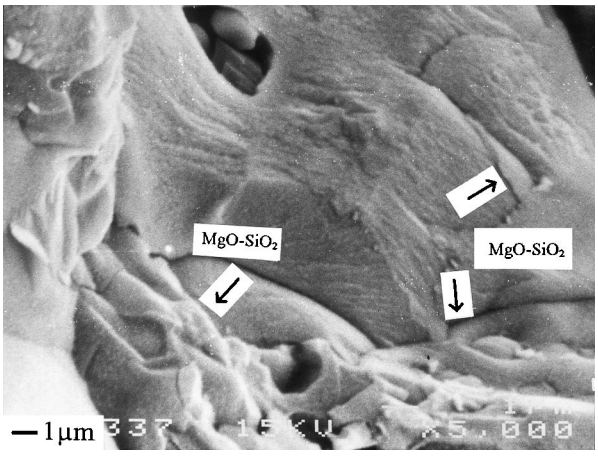

Fig. 11. Cubic zirconia grain surrounded by glassy magnesium silicates, 300–400 μm from the outer area, dense zirconia (mat. A) after corrosion test at 1550°C for 120 min, region I.

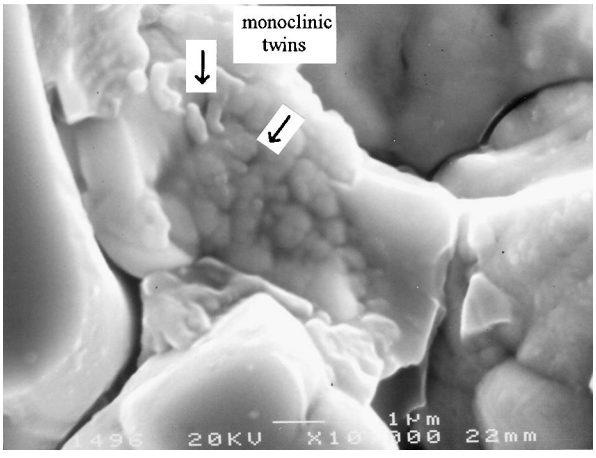

Fig. 12. Monoclinic twins in cubic zirconia grains, 500–600 μm from the outer area, dense zirconia (mat. A) after corrosion test at 1550°C for 120 min, region I.

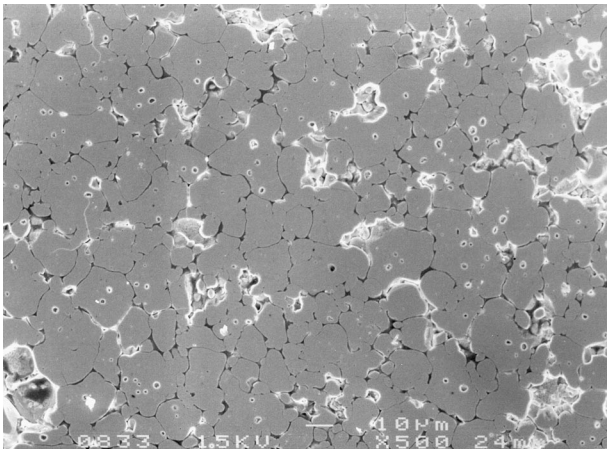

Fig. 13. Polished surface, 600–700 μm from the outer area, reduced phase transformation, dense zirconia (mat. A) after corrosion test at 1550°C for 120 min, region I.

has penetrated and magnesium silicates are identified around the monoclinic grains (Fig. 10). The amount of magnesium silicates increases about 400 μm from the outer surface, with the white regions of Fig. 8 involving phase transformation tetragonal to monoclinic within the cubic grains. Fig. 11 shows zirconia grains surrounded by glassy magnesium silicates.

Fig. 12, 500–600 μm from the outer surface, shows monoclinic twins with size of 0.5–2 μm. The transformation rate is reduced in the region 650–700 μm from the outer surface, Fig. 13. Through XRD analysis a high amount of monoclinic phase has been identified in the inner disagreggated region (before polishing of the specimens) as in the outer area, see Table 3. Also EDX line scans have shown a high amount of Na and Si in the inner disagreggated region as in the slag, Fig. 14(a) and (b). These results indicate a diffusion of Na and Si in the inner area, whereby they drain the MgO stabilising agent out of the crystal and react to magnesium silicates at the grain boundaries. The resulting phase transformation leads to volume expansion and new monoclinic grains with surrounding porosity are produced. The porous structures allow slag penetration, with an active "catalytic" surface for corrosion attack and with dissolution in the slag.

The same attack has been observed at the region ceramic/air/slag, (see Table 3 and Fig. 15). In this case the line scans have shown higher Si amount and less Na in the inner surface, causing phase transformation and disaggregation of the structure, Fig. 14(c) and (d).

Table 3
Phase composition at the different attacked regions on the outer area (direct in contact with slag and steel) and in the inner area (approximately 500 μ from the outer area)

Material A, dense, fine	Region I interface ceramic/steel/slag		Region II interface ceramic/air/slag		Specimen before corrosion
	Outer area	Inner area	Outer area	Inner area	
Monoclinic (vol.%)	49	44	35	34	8
Tetragonal and cubic (vol.%)	51	56	75	76	92

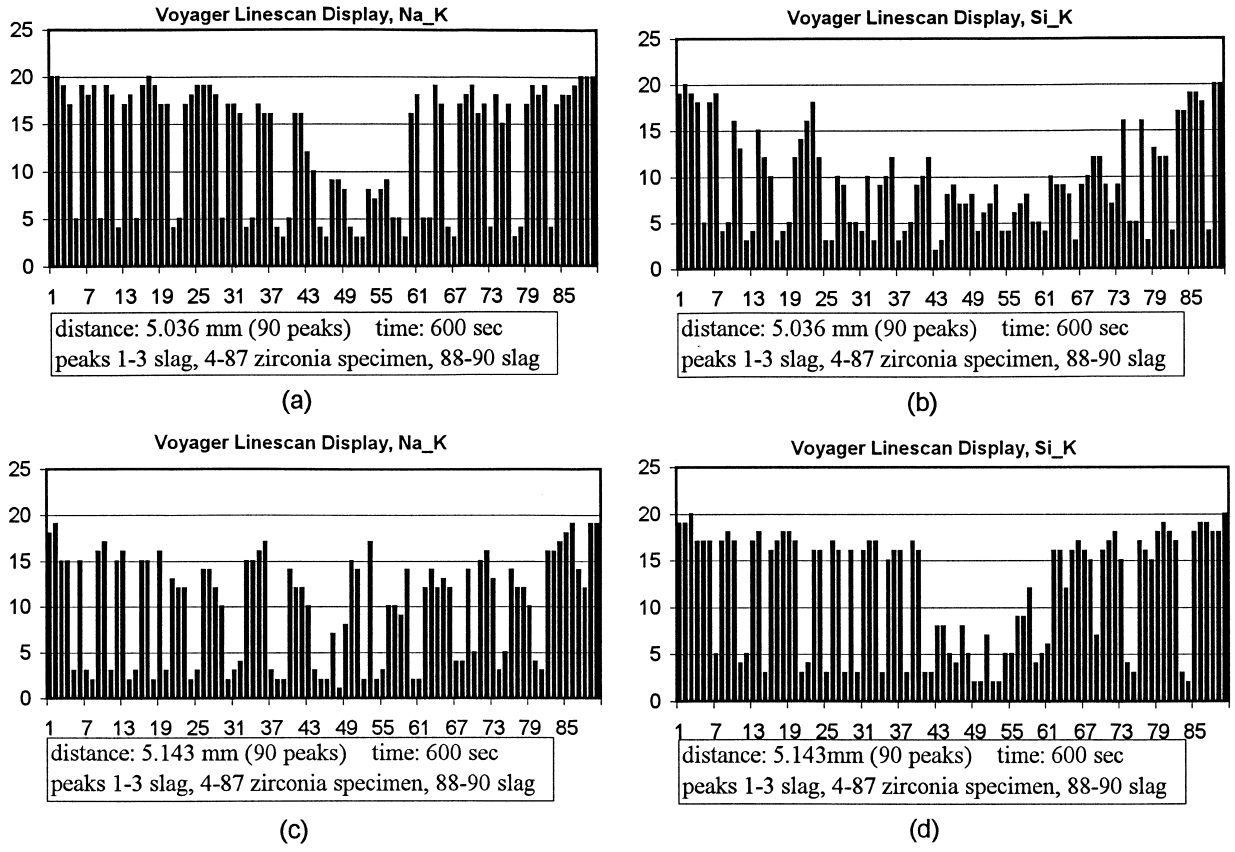

Fig. 14. EDX line scans at a cross section of region I (position 9.3 in Fig. 3) of Na (a) and Si (b) and at a cross-section of region II (position 6.3 in Fig. 3) of Na (c) and Si (d), material A.

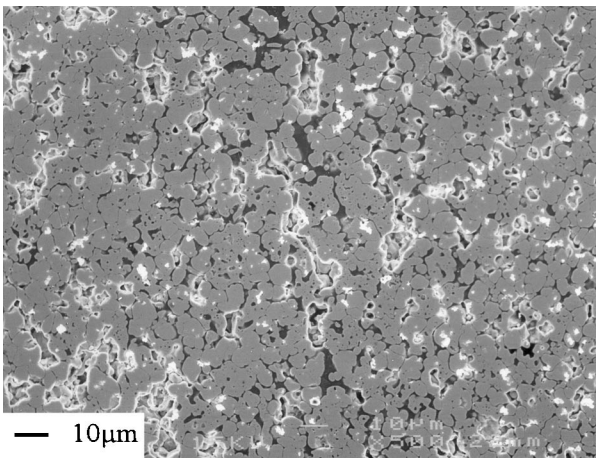

Fig. 15. Region II, cross section of polished surface 200 μm from the outer area, dense zirconia (mat. A) after corrosion test at 1550°C for 120 min.

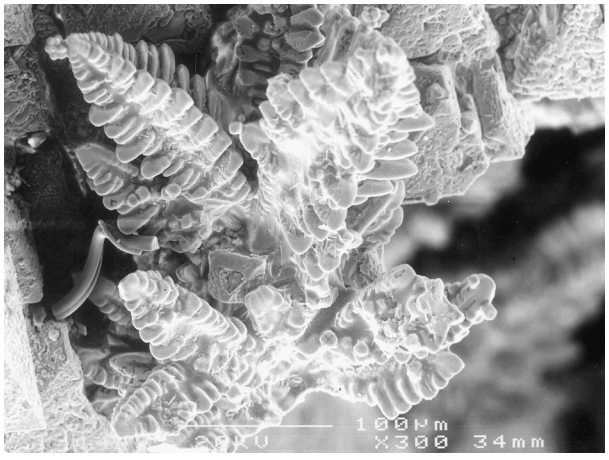

Fig. 16. Partially dissolved zirconia dendrite crystals at the outer area, region I, dense zirconia (mat. A) after corrosion test at 1550°C for 120 min.

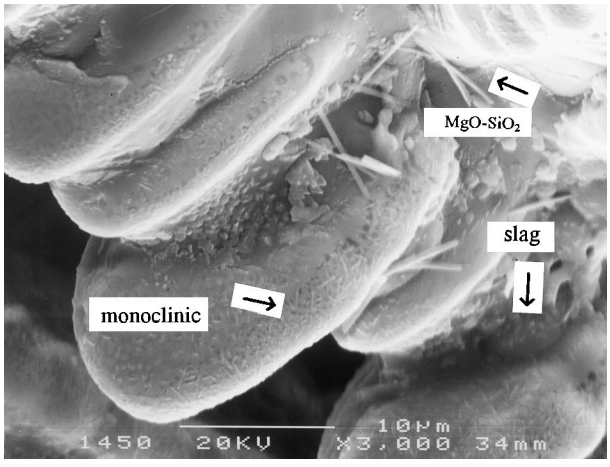

Fig. 17. Dendrite cubic zirconia crystals of Fig. 16 consisting of porous regions with monoclinic twins, mat. A, outer area after corrosion test at 1550°C for 120 min.

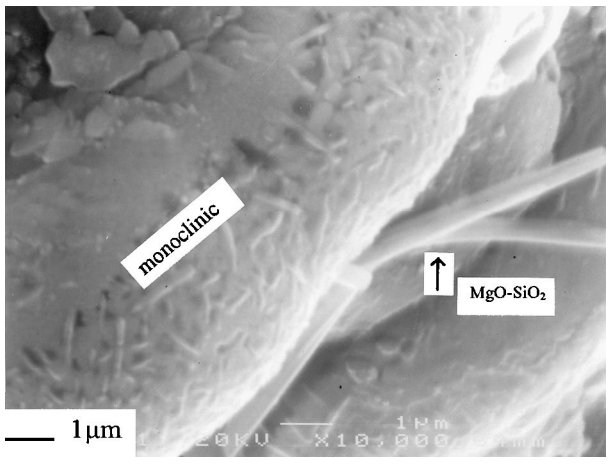

Fig. 18. Detail of Fig. 17 presenting porous regions, monoclinic twins, long fibers of magnesium silicates and slag in cubic grains, region I.

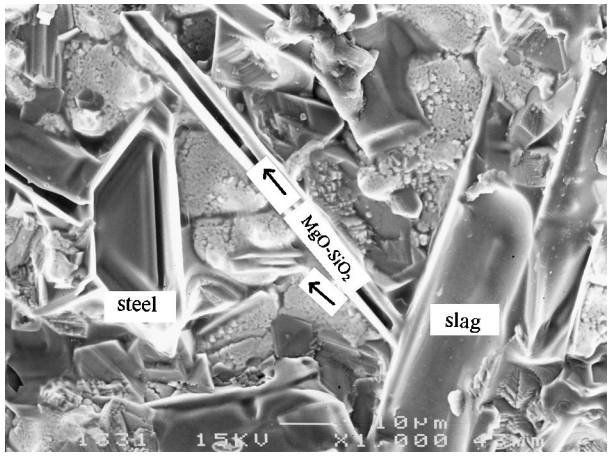

Fig. 19. Porous regions with monoclinic phase surrounded by sharp thin magnesium silicate fibers, slag and molten steel plates, outer area directly in contact with the slag and steel, region I.

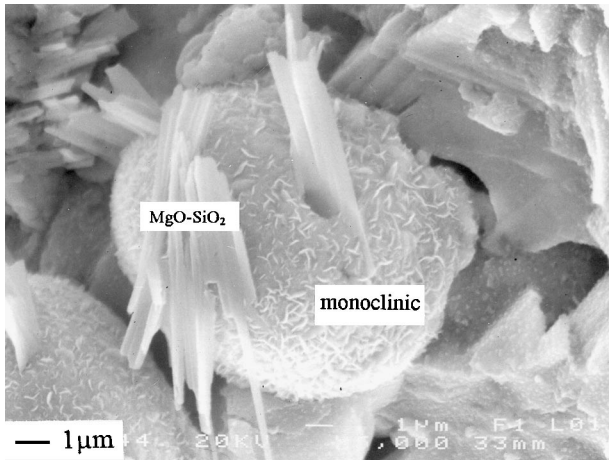

Fig. 20. Monoclinic grains in cubic porous stuctures with sharp magnesium silicate fibers going through the cubic matrix, 50–150 μm from the outer area, region I.

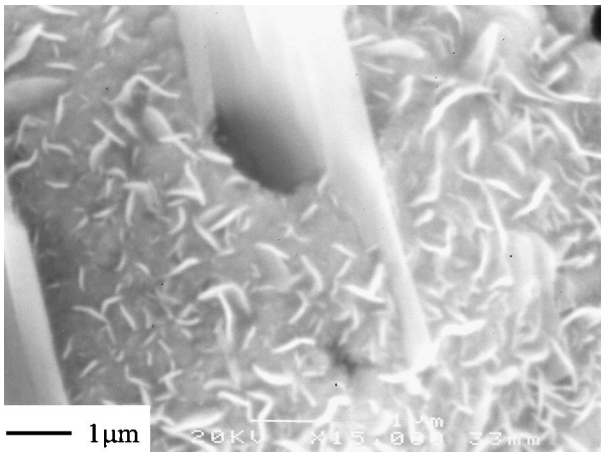

Fig. 21. Detail of Fig. 20.

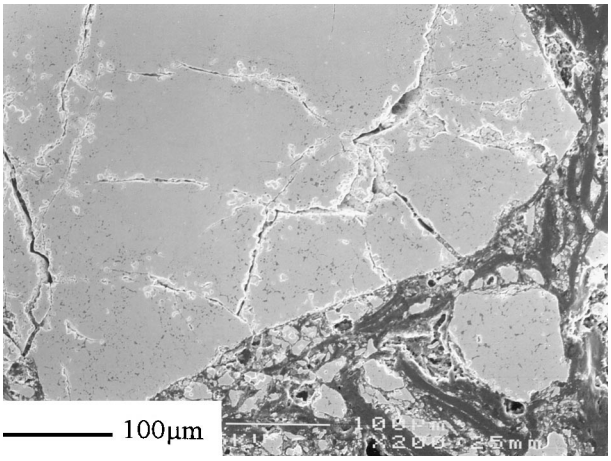

Fig. 22. Cross-section of polished surface of carbon bonded zirconia (mat. C), 600 μm from the outer area, big porous grain (porous regions caused by martensitic transformation) surrounded by magnesium silicates and carbon at the grain boundaries, region I, after corrosion test at 1550°C for 120 min.

In order to observe the corrosion mechanisms three dimensionally details have been obtained through SEM micrographs of broken surfaces. In Fig. 16 the partial dissolved zirconia dendrite crystals can be observed. They consist of porous regions with monoclinic twins in cubic grains (Figs. 17 and 18), whereby they are surrounded by magnesium silicate fibers and slag dark fields. In Fig. 19 the outer area directly in contact with the slag/steel interface is presented. Porous regions of monoclinic grains are surrounded by sharp magnesium silicate fibers, crystallised slag and molten steel plates. Just behind this region 100–200 μm (see also Fig. 9) zirconia monoclinic grains in cubic porous structures are identified with sharp magnesium silicate fibers going through the cubic structure, Figs. 20 and 21.

In Fig. 22 a cross-section region of a carbon bonded zirconia material at a distance 600 μm from the outer attacked area is presented. The big grain is surrounded by magnesium silicates and by carbon at the grain

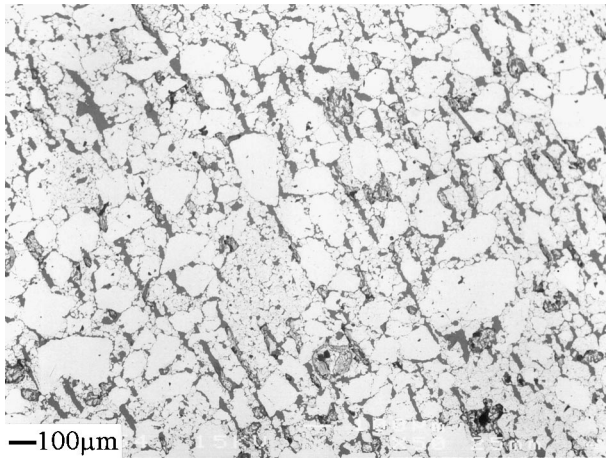

Fig. 23. Cross-section of polished surface of sintered zirconia (mat. B), 600 μm from the outer area, dense and porous cubic grains partially undertaken martensitic transformation, region I, after corrosion test at 1550°C for 120 min.

boundaries. Through the martensitic transformation and the volume expansion of the monoclinic phase the grain has been disaggregated. New free surface and open paths for corrosion attack have resulted. A similar phenomenon has been identified in the 18% porous zirconia material, Fig. 23. In comparison to the dense zirconia, the attacked regions through diffusion of Na and Si are larger and deeper inside of the material. Approximately 2000 μm from the outer surface phase transformation rates have been reduced strongly.

A similar destabilisation process followed by martensitic transformation has been observed in CaO partial stabilised zirconia refractory materials in contact with molten steel and slag.[25] In this case the phase transformation has been identified principally at the outer reaction surface.

4. Conclusions

Corrosion tests of MgO partially stabilised zirconia materials have been carried out in a special designed device simulating the corrosion attack of submerged nozzles during modern continuous steel casting technologies. From these investigations the following conclusions are drawn:

(a) At the outer surface of the ceramic on the interface ceramic/steel/slag local corrosion attack takes place at the grain boundaries through chemical dissolution processes, whereby the amount of porous surface (pores, flaws and cracks resulting from the volume expansion of the martensitic transformation) leads to significant catalytic accelerated reactions.
(b) During the corrosion attack at the outer surface, Na and Si diffuse to the inside of the ceramic.

(c) The slag removes the stabilising agent out of the zirconia crystal to give magnesium silicates at the grain boundaries.
(d) Because of the destabilisation, martensitic phase transformation occurs and volume expansion is caused.
(e) Through the volume expansion, microcracks are introduced in the cubic grains and through serrated planes and uplifts, the microstructure loses its integrity.
(f) The microcracks and the serrated grains create new paths for slag penetration and a porous surface for the catalytic dissolution reactions.

At first sight, it seems that monoclinic zirconia would present an excellent performance according the corrosion attack because no destabilisation could take place. However, considering the manufacture and the poor thermal shock resistance of bulk zirconia components, this is not realistic. Low porosity zirconia components of less than 35% monoclinic phase exhibit an acceptable thermal shock behaviour accompanied by very good corrosion resistance.[26,27] Generally the properties of zirconia materials with amounts of monoclinic phase have to be adapted to the application according to the corrosion and thermal shock requirements. In answering that challenge new testing methods simulating real operating conditions have to be developed.

Zirconia materials suffer also at the interface ceramic/air/slag under corrosion attack. In this case Si diffuses to the inside of the ceramic and disaggregates the structure. This second attacked region should always be carefully examined for mechanical failure of the components (flaw size growth due to volume expansion) or for functional failure (O_2 attack of the molten steel through the microcracks).

Magnesium silicates have been identified at both critical interfaces. Because of the higher amount of Na diffused in the zirconia matrix in the case of the ceramic/steel/slag interface, more glassy magnesium silicate phases have been registered.

Iron and steel, non ferrous metals, cement, chemicals, glass and ceramic producers all depend on refractories to produce their products. Meeting the diverse demands requires understanding of the corrosion mechanisms and of the principles to control the corrosion rates; this opens new horizons for the refractory industry to develop new materials well matched to ecological and economical demands.

References

1. Asano, K. and Ishi, A., Near net shape casting refractories needed to develop it. *Taikabutsu Overseas*, 1991, **71**(1), 50–57.
2. Shirota, Y., Present state subject of tundish metallurgy. *Taikabutsu Overseas*, 1989, **9**(2), 38–46.
3. Krönert, W., Entwicklungstendenzen bei feuerfesten Werkstoffen für den Stranggußbereich. *Proceedings of 29th Internat. Feuerfest Kolloqium Aachen*, 1986, pp. 47–79.
4. Sugita, K., Ikeda, M. and Tamura, S., Microstructural improvements in slide gate plates for steel pouring. *Ceramic Bulletin*, 1984, **63**(7), 886–889.
5. Lax, H., Der Einsatz von feuerfesten Werkstoffen in Stranggießanlagen. *Proceedings of 29th Internat. Feuerfest Kolloqium Aachen*, 1986, pp. 1–46.
6. Krüger, B., Meierling, P., Kappes, H., Dittrich, R. and Corrado, R., Saldanha Steel -die neue Minimill-Produktionslinie für dünne Flacherzeugnisse hoher Qualität. *Stahl und Eisen*, 1997, **117**(11), 80–94.
7. Parbel, W., Schruff, F., Bergmann, B. and Weiler, M., High quality refractory materials–the key to modern continuous casting technology. *Proceedings of 44th Internat. Conference for Continuous Casting Brussel*, 1988, pp. 483–494.
8. Leistner, H., Ratcliffe, D. and Schuler, A., Improved material design devices for continuous casting components. *Proceedings of 2nd Worldwide Conference on Refractories Aachen*, 1991, pp. 316–319.
9. Maier, H. R., Design Management Strukturkeramik. Cfi/Ber. *DKG67*, 1990, **4**, 24.
10. Hiragushi, K., Corrosion of various basic bricks by CaO-SiO_2-Fe_2O_3-MgO slag. *Taikabutsu Overseas*, 1985, **5**(1), 12–20.
11. Ikeksue, A., Wearing test for slag-metal interface and metal zone using high capacity induction furnace. *Taikabutsu Overseas*, 1988, **10**(3), 126–136.
12. Cooper, A. and Kingery, W., *Corrosion of Refractories by Liquid Slags and Glasses*. ed. W. Kingery, MIT, 1959, pp. 85–91.
13. Benedetti, B. and Burlando, G., Corrosion resistance of resin bonded magnesia carbon refractories. *British Ceram. Trans. J.*, 1989, **88**, 55–57.
14. Hauck, F. G., Der Verschleiss von Tauchausgüssen beim Stranggiessen von Stahl. Dissertation Thesis Technical Univ. of Aachen, 1981, pp. 25–55.
15. Refractory materials and their properties, Publisher Didier Werke AG Wiesbaden - Germany, 1990.
16. Hyatt, E. P., Christensen, C. J. and Cutler, I. B., Sintering of zircon and zirconia with the aid of certain additive oxides. *Am. Ceram. Soc. Bull.*, 1957, **36**, 307–309.
17. Stevens, R., An introduction to zirconia. Magnesia Electron publication Shervin Rivers Ltd - England, No. 113, 1983.
18. Kelly, P. M. and Ball, C. J., Crystallography of stress induced martensitic transformation in partially stabilised zirconia. *J. Am. Ceram. Soc.*, 1986, **69**(3), 259–264.
19. Behrens, G., Martinez-Fernandez, J., Dranswaan, G. W. and Heuer, A. H., Isothermal martensitic transformation in ZrO_2 ceramics. Science and technology of Zirconia V, Technomic publication Switzerland, 1993, pp. 3–15.
20. Endres, H. G., Einfluß des Sinterverhaltens und der Gefügeausbildung auf das Ausdehnugs- und Thermoschock-verhalten von ZrO_2-Werkstoffen. Dissertation Thesis Technical Univ. of Aachen, 1985, pp. 18–70.
21. Aneziris, C. G., Pfaff, E. M. and Maier, H. R., Ceramic materials in the system ZrO_2-TiO_2-Al_2O_3 for applications in the ferrous and non ferrous metallurgy. 5th Euro-Ceramics France, Key Engineering Materials 132–136, 1997, 3, pp. 1829–1833.
22. Aneziris, C. G., Pfaff, E. M. and Maier, H. R., Designing principles of ZrO_2-TiO_2-Al_2O_3-MgO based ceramics for refractory applications in the ferrous and nonferrous

metallurgy, *3rd International Refractory Congress IREFCON 98*, Calcutta India, 1998, 2, pp. 339–344.
23. Diaz, M. J. and Edirisinghe, R. B., Characterisation of a zirconia–yttria–titania thermal barrier coating. *J. Mat. Science Letter*, 1994, **13**, 1595–1598.
24. Iwamoto, N. and Umesaki, E. S., Characterisation of plasma — sprayed zirconia coatings by x-ray diffraction and Raman spectroscopy. *Thin Solid Films*, 1985, **127**, 129–137.
25. Oki, K., Sugie, M., Kurihara, K. and Aiba, Y., Wear pattern of zirconia refractories by molten steel and slag. *Proceedings of 2nd Int. Conference on Refractories*, Tokyo, 1987, pp. 721–736.
26. Grimm, N., Verbesserung von dichten Zirkondioxid-Werkstoffen für keramische Bauteile in Verschlußsystemen für den flüssigen Stahl. Dissertation. Thesis Technical Univ. of Aachen, 1993, pp. 82-115.
27. Karaulov, A. G., Grebenyuk, A. A. and Rudyak, I. N., Spalling resistance of zirconia materials. Izo. *Akad. Nauk SSSR, Neorg. Mater*, 1967, **3**, 1101.